

Reconstruction of the wind velocity profile by the intensity fluctuations of a scattered wave in a receiving telescope

V.A. Banakh, D.A. Marakasov

Abstract. The problem of the wind velocity profile reconstruction from random intensity fluctuations of a laser beam diffusely scattered by a screen and received by a telescope is considered. Expressions for a spatiotemporal correlation function and spectrum of weak intensity fluctuations of the reflected beam are presented. An algorithm is proposed for the reconstruction of the profile and direction of the wind velocity from the intensity fluctuation spectra of reflected radiation received by the telescope. The efficiency of the algorithm is confirmed by the results of numerical experiments.

Keywords: optical turbulence, laser beam, reflection, wind profile, reconstruction.

1. Introduction

At present remote probing finds more and more applications in atmospheric studies. In particular, apart from sodars, Doppler lidars are used to study the dynamics of turbulent wind fields in the atmosphere. However, wind lidars, especially with the coherence reception, are very complex, highly technological optoelectronic devices, whose cost of production and maintenance is very high. Simpler and cheaper to realise are the methods based on the results of the statistical processing of optical images of the observed objects or intensity distributions in the cross section of laser beams propagating in the atmosphere.

The problem of measuring the wind velocity by the spatiotemporal statistics of optical wave intensity fluctuations in the turbulent atmosphere was considered in [1] and earlier papers cited in it, where the methods for measuring the path-averaged transverse component of the wind velocity were proposed. The methods have been elaborated recently for estimating the wind velocity profile by the spatiotemporal correlation function of scintillation detection and ranging (SCIDAR) [2–6], which provide the reconstruction of the wind velocity profile and the structural characteristic of the refractive index with a resolution of several hundred meters. An alternative method for the wind

velocity profile reconstruction based on the correlation spectral analysis of intensity fluctuations was proposed in [7, 8].

The problem of determining the wind velocity by the statistics of intensity fluctuations of light scattered by the surface of the observed object was considered in [9], where expressions for estimating the path-average wind velocity were derived. In paper [10], based on the approach presented in [7, 8], an algorithm was developed for reconstructing the velocity profile by the intensity fluctuations of radiation scattered in the focal plane of a receiving telescope, which provided the profile reconstruction on two thirds of the path except the segment adjacent to a diffusely scattering screen.

In this paper we propose the algorithm for calculating the wind velocity profile by the statistics of intensity fluctuations of laser radiation reflected from a diffuse surface and received by a telescope in the case of weak optical turbulence for an arbitrary distance between the detection plane and receiving objective. Expressions for the spatiotemporal correlation function of the intensity fluctuations and its spectrum as well as basic equations for determining the value and direction of the transverse component of the wind velocity are presented. It is shown that the minimal reconstruction error is achieved upon detection of intensity fluctuations in the sharp image plane. Results of numerical experiments confirming the efficiency of the proposed algorithm are presented.

2. Formulation of the problem and basic relations

Let a laser source located in the plane $x = 0$ illuminate a diffusely scattering surface in the plane $x = L$. Scattered radiation propagates through the receiving objective placed in the source plane and is detected by the array of photodetectors (video camera) at a distance l behind the objective. The receiving objective and the source are separated by a distance in the plane $x = 0$ (Fig. 1), which, as shown in [10], allows one to neglect the correlation between the incident and reflected waves and to simplify the reconstruction of the wind velocity profile. Data on the wind velocity on the path between the source and the diffusely scattering surface is extracted from two-dimensional intensity distributions in the detection plane with the help of the correlation spectral analysis.

To calculate the spatiotemporal correlation function

$$K_I(\mathbf{R}, \boldsymbol{\rho}, \tau) = \langle I_r(\mathbf{R} + \boldsymbol{\rho}/2, 0) I_r(\mathbf{R} - \boldsymbol{\rho}/2, \tau) \rangle -$$

V.A. Banakh, D.A. Marakasov Institute of Atmospheric Optics, Siberian Branch, Russian Academy of Sciences, prosp. Akademicheskii 1, 634055 Tomsk, Russia; e-mail: banakh@iao.ru, mda@iao.ru

Received 24 August 2007; revision received 12 February 2008
Kvantovaya Elektronika 38 (9) 889–894 (2008)
Translated by I.A. Ulitkin

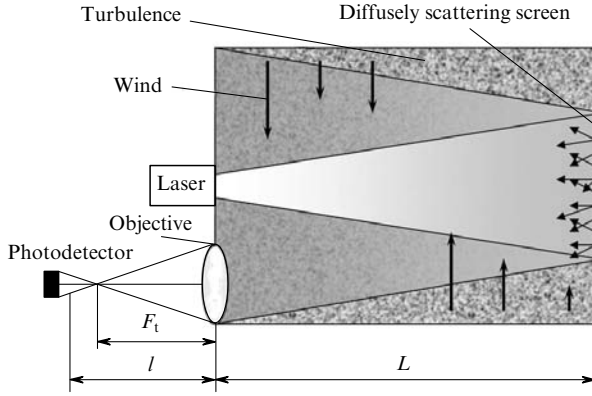


Figure 1. Geometry of the problem of the wind velocity profile reconstruction.

$$-\langle I_r(\mathbf{R} + \boldsymbol{\rho}/2, 0) \rangle \langle I_r(\mathbf{R} - \boldsymbol{\rho}/2, \tau) \rangle, \quad (1)$$

where $I_r(\boldsymbol{\rho}, t)$ is the intensity in the detection plane $x = -l$ at the instant t ; τ is the temporal shift; $\mathbf{R}, \boldsymbol{\rho}$ are the vectors perpendicular to the optical axis, we will assume that the fluctuations of the diffuse reflectance from the surface are independent of fluctuations of the dielectric constant of the air. By assuming that the time scale of reflectance fluctuations is smaller than the interval between the frames, the values of the reflectance at different instants of time can be treated as independent. This allows one to replace instant intensities in (1) by their values averaged over fluctuations of the reflectance. In accordance with [11], the expression for the intensity averaged over the reflectance in the detection plane can be written in the form

$$I_r(\boldsymbol{\rho}, t) = \frac{1}{\pi l^2} \int d\mathbf{r} |A(\mathbf{r})|^2 I_i(\mathbf{r}, t) I_t(\mathbf{r}, \boldsymbol{\rho}, t), \quad (2)$$

where we will describe the amplitude of the scattering coefficient $A(\mathbf{r})$ by a Gaussian:

$$A(\mathbf{r}) = A_0 \exp\left(-\frac{r^2}{2a_r^2}\right), \quad (3)$$

where A_0 is the amplitude at the centre of a diffuse reflector; and a_r is the effective radius of the reflector. The integrand in (2) contains the intensity I_i of a laser beam illuminating the diffuse surface and the intensity I_t of the additional (telescopic) beam, whose parameters are determined by the objective characteristics. A telescopic beam is produced by a point source with the unit amplitude, which is located at the point $\boldsymbol{\rho}$ of the detection plane, and propagates along the same path as the illuminating beam. One can say that the illuminated region of the diffuse surface is 'scanned' by this beam. The intensities I_i and I_t can be calculated from expressions

$$I_i(\mathbf{r}, t) = \left| \int d\boldsymbol{\rho}_1 U_i(0, \boldsymbol{\rho}_1) G(L, \mathbf{r}; 0, \boldsymbol{\rho}_1; t) \right|^2, \quad (4)$$

$$I_t(\mathbf{r}, \boldsymbol{\rho}, t) = \left| \int d\boldsymbol{\rho}_2 T(\boldsymbol{\rho}_2) \exp\left[\frac{ik}{2} \left(\frac{1}{l} - \frac{1}{F_t}\right) \boldsymbol{\rho}_2^2 - \frac{ik}{l} \boldsymbol{\rho} \boldsymbol{\rho}_2\right] \times G(L, \mathbf{r}; 0, \boldsymbol{\rho}_2; t) \right|^2, \quad (5)$$

where

$$U_i(0, \boldsymbol{\rho}) = U_0 \exp\left(-\frac{\rho^2}{2a_0^2} - \frac{ik}{2F_0} \rho^2\right) \quad (6)$$

is the complex field amplitude of a laser source in the plane $x = 0$; a_0 and F_0 are the beam radius and the radius of the wave-front curvature, respectively; $k = 2\pi/\lambda$; λ is the wavelength; U_0 is the field amplitude on the optical axis; $T(\boldsymbol{\rho}_2)$ is the objective transmission function for which we will use the Gaussian approximation

$$T(\boldsymbol{\rho}_2) = T_0 \exp\left(-\frac{\rho_2^2}{2a_t^2}\right); \quad (7)$$

F_t is the focal length of the objective; a_t is its effective radius. It is convenient to write the Green function in the form of the product of regular and random components ([12], p. 17):

$$G(L, \mathbf{r}; 0, \boldsymbol{\rho}; t) = G_0(L, \mathbf{r}; \boldsymbol{\rho}; t) G_r(L, \mathbf{r}; 0, \boldsymbol{\rho}; t). \quad (8)$$

The regular component $G_0(L, \mathbf{r}; \boldsymbol{\rho}; t) = (i\lambda L)^{-1} \exp[ik(\mathbf{r} - \boldsymbol{\rho})^2 \times (2L)^{-1}]$ represents the Green function of the homogeneous medium in the paraxial approximation. The random component $G_r(L, \mathbf{r}; 0, \boldsymbol{\rho}; t)$ taking into account the fluctuations of the refractive index on the path, can be represented in the form of a continual integral [13]:

$$G_r(L, \mathbf{r}; 0, \boldsymbol{\rho}; t) = \lim_{N \rightarrow \infty} \left(\frac{k}{2\pi i L}\right)^{N-1} \int d\mathbf{S}_1 \dots \int d\mathbf{S}_{N-1} \times \exp\left(\frac{ik}{2L} \sum_{j=1}^{N-1} S_j^2\right) \exp\left\{\frac{ikL}{2} \int_0^1 d\xi \times \varepsilon_1\left(\xi L, (1-\xi)\boldsymbol{\rho} + \xi\mathbf{r} + \sum_{j=1}^{N-1} v_j(\xi) \mathbf{S}_j\right)\right\}, \quad (9)$$

where $\varepsilon_1(x, \boldsymbol{\rho})$ is the random component of the dielectric constant of the air; \mathbf{S}_j are two-dimensional vectors perpendicular to the optical axis; $\xi = x/L$; $v_j(\xi) = \sin(j\pi\xi) \times [\sqrt{2N} \sin(j\pi/2N)]^{-1}$.

The substitution of (2) with the use of (3)–(9) in (1) allows one to write the expression for the correlation intensity function, in which in front of the integral of the same type as in the second exponent in (9) the parameter $\beta_0^2 = 1.23 C_n^2 k^{7/6} L^{11/6}$, characterising the turbulent propagation conditions appears, where C_n^2 is the structural characteristic of refractive index fluctuations. We will consider below the regime of weak optical turbulence, when the parameter β_0^2 does not exceed the unity. In this case, we can restrict consideration by the first significant term in the expansion of correlation function (1) in series by intensity fluctuations:

$$K_I(\mathbf{R}, \boldsymbol{\rho}, \tau) = \frac{1}{\pi^2 l^4} \int d\mathbf{r}_1 \int d\mathbf{r}_2 |A(\mathbf{r}_1) A(\mathbf{r}_2)|^2 \times \left[I_{i0}\left(\mathbf{r}_1, \mathbf{R} + \frac{\boldsymbol{\rho}}{2}\right) I_{i0}\left(\mathbf{r}_2, \mathbf{R} - \frac{\boldsymbol{\rho}}{2}\right) K_{I_i}\left(\frac{\mathbf{r}_1 + \mathbf{r}_2}{2}, \mathbf{r}_1 - \mathbf{r}_2; \tau\right) + I_{i0}(\mathbf{r}_1) I_{i0}(\mathbf{r}_2) K_{I_t}\left(\frac{\mathbf{r}_1 + \mathbf{r}_2}{2}, \mathbf{r}_1 - \mathbf{r}_2; \mathbf{R}, \boldsymbol{\rho}; \tau\right) \right], \quad (10)$$

where due to the spatial separation of the transmitter and the receiving objective in the plane $x = 0$ we neglected the mutual correlation of intensity fluctuations of illuminating (4) and additional (5) beams. The functions $I_{i0}(\mathbf{r})$ and $I_{i0}(\mathbf{r}, \boldsymbol{\rho})$ are unperturbed intensity profiles of illuminating and additional beams, respectively, i.e. calculated in the absence of the refractive index fluctuations. In the reflector plane expressions for them can be written in the form

$$I_{i0}(\mathbf{r}) = \frac{k^2 U_0^2}{|z_i|^2 L^2} \exp\left(-\frac{k^2 r^2}{a_0^2 |z_i|^2 L^2}\right),$$

$$I_{i0}(\mathbf{r}, \boldsymbol{\rho}) = \frac{k^2 T_0^2}{|z_i|^2 L^2} \exp\left[-\frac{k^2}{a_i^2 |z_i|^2 L^2} \left(\mathbf{r} + \frac{L}{l} \boldsymbol{\rho}\right)^2\right], \quad (11)$$

where notations

$$z_i = -\frac{1}{a_0^2} + ik\left(\frac{1}{L} - \frac{1}{F_0}\right), z_t = -\frac{1}{a_t^2} + ik\left(\frac{1}{L} + \frac{1}{l} - \frac{1}{F_t}\right) \quad (12)$$

are introduced.

To calculate the correlation functions

$$K_{I_i}\left(\frac{\mathbf{r}_1 + \mathbf{r}_2}{2}, \mathbf{r}_1 - \mathbf{r}_2; \tau\right) = \langle I_i(\mathbf{r}_1, 0) I_i(\mathbf{r}_2, \tau) \rangle$$

$$-\langle I_i(\mathbf{r}_1) \rangle \langle I_i(\mathbf{r}_2) \rangle = \left(\frac{k^2 U_0}{4\pi^2 L^2}\right)^2 \int d\boldsymbol{\rho}_1 \int d\boldsymbol{\rho}_2 \int d\boldsymbol{\rho}_3 \int d\boldsymbol{\rho}_4$$

$$\times \Gamma_{r4}(\mathbf{r}_1, \mathbf{r}_2; \boldsymbol{\rho}_{1-4}; \tau) \exp\left[\frac{z_i}{2}(\rho_1^2 + \rho_3^2) + \frac{z_i^*}{2}(\rho_2^2 + \rho_4^2)\right.$$

$$\left. - \frac{ik}{L} \mathbf{r}_1(\boldsymbol{\rho}_1 - \boldsymbol{\rho}_2) + \frac{ik}{L} \mathbf{r}_2(\boldsymbol{\rho}_3 - \boldsymbol{\rho}_4)\right], \quad (13)$$

$$K_{I_t}\left(\frac{\mathbf{r}_1 + \mathbf{r}_2}{2}, \mathbf{r}_1 - \mathbf{r}_2; \mathbf{R}, \boldsymbol{\rho}; \tau\right) = \left\langle I_t\left(\mathbf{r}_1, \mathbf{R} + \frac{\boldsymbol{\rho}}{2}, 0\right)\right.$$

$$\left. \times I_t\left(\mathbf{r}_2, \mathbf{R} - \frac{\boldsymbol{\rho}}{2}, \tau\right)\right\rangle - \left\langle I_t\left(\mathbf{r}_1, \mathbf{R} + \frac{\boldsymbol{\rho}}{2}\right)\right\rangle \left\langle I_t\left(\mathbf{r}_2, \mathbf{R} - \frac{\boldsymbol{\rho}}{2}\right)\right\rangle$$

$$= \left(\frac{k^2 T_0}{4\pi^2 L^2}\right)^2 \int d\boldsymbol{\rho}_1 \int d\boldsymbol{\rho}_2 \int d\boldsymbol{\rho}_3 \int d\boldsymbol{\rho}_4 \Gamma_{r4}(\mathbf{r}_1, \mathbf{r}_2; \boldsymbol{\rho}_{1-4}; \tau)$$

$$\times \exp\left[\frac{z_t}{2}(\rho_1^2 + \rho_3^2) + \frac{z_t^*}{2}(\rho_2^2 + \rho_4^2) - \frac{ik}{l} \left(\mathbf{R} + \frac{\boldsymbol{\rho}}{2}\right)\right.$$

$$\left. + \frac{l}{L} \mathbf{r}_1(\boldsymbol{\rho}_1 - \boldsymbol{\rho}_2) + \frac{ik}{l} \left(\mathbf{R} - \frac{\boldsymbol{\rho}}{2} + \frac{l}{L} \mathbf{r}_2\right)(\boldsymbol{\rho}_3 - \boldsymbol{\rho}_4)\right] \quad (14)$$

of illuminating and telescopic beams, respectively, it is necessary to determine the fourth moment of the random component of the Green function

$$\Gamma_{r4}(\mathbf{r}_1, \mathbf{r}_2; \boldsymbol{\rho}_{1-4}; \tau) = \langle G_r(L, \mathbf{r}_1; 0, \boldsymbol{\rho}_1; 0) G_r^*(L, \mathbf{r}_1; 0, \boldsymbol{\rho}_2; 0)$$

$$\times G_r(L, \mathbf{r}_2; 0, \boldsymbol{\rho}_3; \tau) G_r^*(L, \mathbf{r}_2; 0, \boldsymbol{\rho}_4; \tau) \rangle$$

$$- \langle G_r(L, \mathbf{r}_1; 0, \boldsymbol{\rho}_1; 0) G_r^*(L, \mathbf{r}_1; 0, \boldsymbol{\rho}_2; 0) \rangle$$

$$\times \langle G_r(L, \mathbf{r}_2; 0, \boldsymbol{\rho}_3; \tau) G_r^*(L, \mathbf{r}_2; 0, \boldsymbol{\rho}_4; \tau) \rangle. \quad (15)$$

We will seek for it similarly to papers [7, 8, 10], by assuming that the relative dispersion of intensity fluctuations does not exceed the unity and by using the hypothesis of the ‘frozen’ Taylor turbulence [14]:

$$\varepsilon_1(x, \boldsymbol{\rho}; \tau) = \varepsilon_1(x, \boldsymbol{\rho} - \mathbf{V}(x)\tau; 0) \quad (16)$$

to describe the spatiotemporal fluctuations of the refractive index, where $V(x)$ is the wind velocity component perpendicular to the direction of radiation propagation. As a result, we obtain

$$\Gamma_{r4}(\mathbf{r}_1, \mathbf{r}_2; \boldsymbol{\rho}_{1-4}; \tau) = k^2 L \int_0^1 d\xi C_n^2(L\xi) \int d\boldsymbol{\kappa} \Phi_n(\boldsymbol{\kappa})$$

$$\times \exp\{i\boldsymbol{\kappa}[\mathbf{V}(\xi L)\tau + \xi \boldsymbol{\Delta}]\} \left\{ \exp[i\boldsymbol{\kappa}(1 - \xi)(\boldsymbol{\rho}_2 - \boldsymbol{\rho}_3)]\right.$$

$$+ \exp[i\boldsymbol{\kappa}(1 - \xi)(\boldsymbol{\rho}_1 - \boldsymbol{\rho}_4)] - \exp\left[i\boldsymbol{\kappa}(1 - \xi)(\boldsymbol{\rho}_1 - \boldsymbol{\rho}_3)\right.$$

$$- i \frac{L}{k} \xi(1 - \xi)\boldsymbol{\kappa}^2] - \exp\left[i\boldsymbol{\kappa}(1 - \xi)(\boldsymbol{\rho}_2 - \boldsymbol{\rho}_4)\right.$$

$$\left. \left. + i \frac{L}{k} \xi(1 - \xi)\boldsymbol{\kappa}^2\right]\right\}, \quad (17)$$

where $\boldsymbol{\Delta} = \mathbf{r}_1 - \mathbf{r}_2$; $\Phi_n(\boldsymbol{\kappa})$ is the three-dimensional spectrum of the refractive index.

The substitution of (17) into (13), (14) with the following integration in the plane $x = 0$ yields the expressions for the correlation functions of illuminating and telescopic beams:

$$K_{I_i}(\mathbf{r}_0, \boldsymbol{\Delta}, \tau) = 2k^2 L I_{i0}\left(\mathbf{r}_0 + \frac{\boldsymbol{\Delta}}{2}\right) I_{i0}\left(\mathbf{r}_0 - \frac{\boldsymbol{\Delta}}{2}\right)$$

$$\times \int_0^1 d\xi \int d\boldsymbol{\kappa} C_n^2(L\xi) \Phi_n(\boldsymbol{\kappa}) \operatorname{Re}\{\exp\{i\boldsymbol{\kappa}[\mathbf{V}(L\xi)\tau + \xi \boldsymbol{\Delta}]\}$$

$$\times [\exp(-\operatorname{Re}\beta_i \boldsymbol{\kappa}^2 - 2\operatorname{Re}\gamma_i \mathbf{r}_0 \boldsymbol{\kappa} + i\operatorname{Im}\gamma_i \boldsymbol{\kappa} \boldsymbol{\Delta})$$

$$- \exp(-\beta_i \boldsymbol{\kappa}^2 + \gamma_i \boldsymbol{\kappa} \boldsymbol{\Delta})]\}, \quad (18)$$

$$K_{I_t}(\mathbf{r}_0, \boldsymbol{\Delta}; \mathbf{R}, \boldsymbol{\rho}; \tau) = 2k^2 L I_{t0}\left(\mathbf{r}_0 + \frac{\boldsymbol{\Delta}}{2}, \mathbf{R} + \frac{\boldsymbol{\rho}}{2}\right)$$

$$\times I_{t0}\left(\mathbf{r}_0 - \frac{\boldsymbol{\Delta}}{2}, \mathbf{R} - \frac{\boldsymbol{\rho}}{2}\right) \int_0^1 d\xi \int d\boldsymbol{\kappa} C_n^2(L\xi) \Phi_n(\boldsymbol{\kappa})$$

$$\times \operatorname{Re}\{\exp\{i\boldsymbol{\kappa}[\mathbf{V}(L\xi)\tau + \xi \boldsymbol{\Delta}]\} [\exp(-\operatorname{Re}\beta_t \boldsymbol{\kappa}^2 - 2\operatorname{Re}\gamma_t \mathbf{r}_0' \boldsymbol{\kappa}$$

$$+ i\operatorname{Im}\gamma_t \boldsymbol{\kappa} \boldsymbol{\Delta}') - \exp(-\beta_t \boldsymbol{\kappa}^2 + \gamma_t \boldsymbol{\kappa} \boldsymbol{\Delta}')]\}, \quad (19)$$

where $\mathbf{r}_0 = (\mathbf{r}_1 + \mathbf{r}_2)/2$; $\mathbf{r}_0' = \mathbf{r}_0 + \mathbf{R}L/l$; $\boldsymbol{\Delta}' = \boldsymbol{\Delta} + \boldsymbol{\rho}L/l$;

$$\beta_{i,t} = i \frac{L}{k} (1 - \xi) \left[\xi + \frac{ik}{Lz_{i,t}} (1 - \xi) \right]; \quad (20)$$

$$\gamma_{i,t} = -\frac{k}{Lz_{i,t}} (1 - \xi). \quad (21)$$

The substitution of expressions for the intensities of the illuminating and additional beams in the absence of

fluctuations (11) and their correlation functions (18), (19) into (10) makes it possible to calculate the integrals by the surface of a diffusely scattering screen and to derive the final expression for the spatiotemporal correlation function of the measured intensity:

$$K_I(\mathbf{R}, \rho, \tau) = K_0 \exp\left(-\frac{2R^2 + \rho^2/2}{a^2}\right) \int_0^1 d\xi \\ \times \int d\mathbf{\kappa} C_n^2(L\xi) \Phi_n(\mathbf{\kappa}) \operatorname{Re}\left\{\exp[i\mathbf{\kappa}\mathbf{V}(L\xi)\tau] \right. \\ \times \sum_{m=1}^2 [\exp(-\operatorname{Re}\beta_m \kappa^2 - 2\operatorname{Re}\gamma_m \mathbf{R}\mathbf{\kappa} + i\operatorname{Im}\gamma_m \rho\mathbf{\kappa}) \\ \left. - \exp(-\beta_m \kappa^2 + \gamma_m \rho\mathbf{\kappa})\right\}, \quad (22)$$

where the following notations are used:

$$K_0 = 2k^2 L \left(\frac{k^2 a_s A_0 U_0 T_0}{l L^2 |z_i z_t|}\right)^4; \quad (23)$$

$$\beta_{1(2)} = \beta_{i(t)} - \frac{a_s^2}{2} (i\xi + \gamma_{i(t)})^2; \quad (24)$$

$$\gamma_1 = -\frac{L a_s^2}{l a_{td}^2} (i\xi + \gamma_i); \quad \gamma_2 = \frac{L}{l} \gamma_t - \frac{L a_s^2}{l a_{td}^2} (i\xi + \gamma_t); \quad (25)$$

$$a_{td} = a_t |z_t| \frac{L}{k}; \quad a_s = \left(a_r^{-2} + a_{td}^{-2} + \frac{k^2}{L^2 a_0^2 |z_i|^2}\right)^{-2}; \quad (26)$$

$$a = \frac{l}{L} \frac{a_{td}}{(1 - a_s^2/a_{td}^2)^{1/2}}.$$

3. Algorithm of the wind velocity profile reconstruction

To reconstruct the wind velocity profile, consider the Fourier transform of correlation function (22). Each of the terms in the right-hand part of (22) differs from the intensity correlation function of the illuminating beam on the straight path only by the values of the parameters $\beta_{1,2}$, $\gamma_{1,2}$ and the effective radius a . Therefore, the spatiotemporal spectrum of the intensity correlation function in the photodetector plane will be analysed similarly to paper [8], where the propagation of a Gaussian beam along a straight path is considered. The spectrum of the refractive index is assumed to be the Kolmogorov one: $\Phi_n(\mathbf{\kappa}) = 0.033\kappa^{-11/3}$. To find the profile of the wind velocity projection on one of the axes of the Cartesian coordinate system with a unit vector \mathbf{e}_i ($i = y, z$), it is convenient to introduce the normalised two-dimensional spatiotemporal spectrum

$$g_i(\omega, q) = \frac{q a^{10/3}}{2^{20/3} \pi^5 K_0 \Phi_n(\mathbf{q})} \int d\mathbf{R} \int d\rho \int d\tau K_I(\rho, \mathbf{R}, \tau) \\ \times \exp[i(\omega\tau + \mathbf{q}\mathbf{e}_i\rho)] = \exp\left(-\frac{q^2 a^2}{2}\right) \int_0^1 d\xi C_n^2(L\xi) \times$$

$$\times \sum_{m=1}^2 \left| \frac{\operatorname{Im}\gamma_m}{\operatorname{Re}\eta_m} \right|^{-11/3} \delta\left(\alpha - \frac{a^2 \operatorname{Im}\gamma_m}{2\operatorname{Re}\eta_m} V_i(\xi L)\right) \\ \times \left\{ \frac{1}{\operatorname{Re}\eta_m} \exp\left[\frac{q^2 a^4 (\operatorname{Im}\gamma_m)^2}{4\operatorname{Re}\eta_m}\right] - \frac{1}{|\eta_m|} \right. \\ \left. \times \exp\left[-\frac{q^2 a^4}{4} \operatorname{Re}\left(\frac{\gamma_m^2}{\eta_m}\right)\right] \cos\left[\frac{q^2 a^4}{4} \operatorname{Im}\left(\frac{\gamma_m^2}{\eta_m}\right) + \arg\eta_m\right] \right\}, \quad (27)$$

where the vector \mathbf{q} of spatial frequencies is oriented along the separated axis: $\mathbf{q} = q\mathbf{e}_i$; $V_i(\xi L) = \mathbf{V}(\xi L)\mathbf{e}_i$ is the projection of the velocity vector on this axis; $\alpha = q/\omega$; $\eta_{1,2} = \beta_{1,2} - a^2 \gamma_{1,2}^2/2$. The introduction of the auxiliary function

$$f_i(\alpha, p) = 4 \int_0^\infty g_i(\alpha, q) \exp(ipq^2) q dq = \int_0^1 d\xi C_n^2(L\xi) \\ \times \sum_{m=1}^2 \left| \frac{\operatorname{Im}\gamma_m}{\operatorname{Re}\eta_m} \right|^{-11/3} \delta\left(\alpha - \frac{a^2 \operatorname{Im}\gamma_m}{2\operatorname{Re}\eta_m} V_i(\xi L)\right) \\ \times \left\{ \frac{2}{\operatorname{Re}\eta_m} \left[\frac{a^2}{2} \left(1 - \frac{a^2 (\operatorname{Im}\gamma_m)^2}{2\operatorname{Re}\eta_m}\right) - ip\right]^{-1} - \frac{1}{\eta_m} \right. \\ \left. \times \left[\frac{a^2}{2} \left(1 + \frac{a^2 \gamma_m^2}{2\eta_m}\right) - ip\right]^{-1} - \frac{1}{\eta_m^*} \left[\frac{a^2}{2} \left(1 + \frac{a^2 \gamma_m^{*2}}{2\eta_m^*}\right) - ip\right]^{-1} \right\} \quad (28)$$

allows one to assign to each point of the path two maxima of the absolute quantity $|f_i(\alpha, p)|$ in the region $p > 0$, which appear when the argument of the delta function tends to zero in (28)

$$\alpha = \alpha_m = \frac{a^2 \operatorname{Im}\gamma_m}{2\operatorname{Re}\eta_m} V_i(\xi L). \quad (29)$$

In the maxima, the imaginary part of the denominator of one of the fractions is close to zero and all the other terms change rather slowly compared to it. We will find the coordinate of the maximum by neglecting these changes in its vicinity:

$$p_{1,2} \approx \frac{a^4}{4} \operatorname{Im} \frac{\gamma_{1,2}^2}{\eta_{1,2}}. \quad (30)$$

The wind velocity profile reconstruction by the coordinates of the maxima of the absolute quantity of auxiliary function (28) is prevented by the fact that it is unknown *a priori* which index m corresponds to the maximum determined by processing the spectrum of the intensity fluctuations. The maxima can be distinguished by choosing the transmission conditions, i.e. parameters of the laser beam and receiver.

Let the illuminating beam be collimated ($F_0 \rightarrow \infty$) and its radius exceed significantly the Fresnel radius ($\delta = (L/k)^{1/2} a_0^{-1} \ll 1$). The photodetector will be placed in the plane of the sharp image ($1/F_t = 1/l + 1/L$) of the receiving objective whose radius is also larger than the Fresnel one. The diffusely scattering screen will be considered infinite ($a_r = \infty$). The coordinates of the maxima will be estimated by restricting consideration by the first significant term in the expansion in the small parameter δ :

$$p_1 \approx \frac{l^2}{kL}(1 - \xi), \quad \alpha_1 \approx -\frac{l}{L} V_i(\xi L), \quad (31)$$

$$p_2 \approx \frac{l^2}{kL} \frac{M^2(1 - \xi)^3 \xi}{[(1 - \xi)^2 M^2 + \xi^2]^2}, \quad (32)$$

$$\alpha_2 \approx -\frac{l}{L} \frac{\xi}{(1 - \xi)^2 M^2 + \xi^2} V_i(\xi L),$$

where $M = a_i/a_0$ is the ratio of the effective radii of the objective and the illuminating beam. The increase ($M \rightarrow \infty$) in the objective size leads to the fact that coordinates p_2 and α_2 tend to zero, while coordinates p_1 and α_1 remain constant and coincide with the positions of the maxima for the plane wave on the straight path with the accuracy to constant factors $(l/L)^2$ and l/L , respectively [7]. Thus, the selection of the receiving objective radius allows one to single out the maxima corresponding to the index $m = 1$, i.e. to establish one-to-one correspondence between the maxima of the absolute quantity of auxiliary function (28) in the region $p > 0$ and the coordinate of the point on the path. By finding the maxima $|f_i(\alpha, p)|$ and solving Eqns (31) with respect to ξ and $V_i(\xi L)$, the profiles of the wind velocity projection $V_i(x)$ can be reconstructed.

4. Numerical experiments on the reconstruction of the wind velocity profile

To calculate the projections of the spatiotemporal spectrum $g_i(\omega, q)$, the laser beam propagation in the turbulent atmosphere and its scattering by a diffusely scattering screen were computer simulated. The atmospheric inhomogeneities were simulated by perturbing the propagating wave by equally-spaced random phase screens with the Kolmogorov spectrum of phase fluctuations. The parameters of the screens and their number were chosen so that to provide the necessary simulation accuracy and to realise the regime of weak fluctuations. The propagation of the illuminating beam was simulated in accordance with the algorithm developed in [15]. To calculate the field of the wave diffusely scattered by the screen, the approximate algorithm proposed in [11] was used.

The transverse component of the wind velocity on the path was simulated by the transverse displacements of the phase screens in time by the distance $V(x)\tau$. The obtained realisations of the intensity in the photodetector plane were processed in accordance with expressions (27), (28), after which the wind velocity profile was determined by the coordinates of the maxima of the functions $|f_i(\alpha, p)|$.

To verify the efficiency of the proposed algorithm, numerical experiments were performed by using a closed scheme. In the first experiment the following parameters were specified: the path length $L = 1000$ m, the wavelength $\lambda = 0.5 \mu\text{m}$, $C_n^2 = 4 \times 10^{-17} \text{m}^{-2/3}$, the effective radius of the diffuse reflector $a_r = \infty$, the focal length of the objective $F_t = 1$ m, its effective radius $a_t = 10$ cm. The photodetector was located in the plane of the sharp image at a distance of 1 mm from the focal plane and the laser beam was collimated with the initial radius $a_0 = 5$ cm. The propagation of the beam in the atmosphere ($0 \leq x \leq L$) was simulated on a grid of size 512×512 elements with a spatial step of 1 mm. The computational grid with the

compression coefficient $L/l \approx 10^3$ was scaled in the photodetector plane. The spectrum was estimated by twenty realisations of the intensity distributions of duration equal to 256 counts with an interval of 1 ms. Figure 2 shows the results of calculations of spatiotemporal spectrum (27). Each phase screen is shown as a beam along which the spectral density has significantly larger values than in its vicinity. Figure 3a presents the results of the wind velocity profile reconstruction. The coordinates and velocities of the transverse displacement of phase screens are reconstructed with errors not exceeding 40 m over the coordinate and 0.1 m s^{-1} over the velocity.

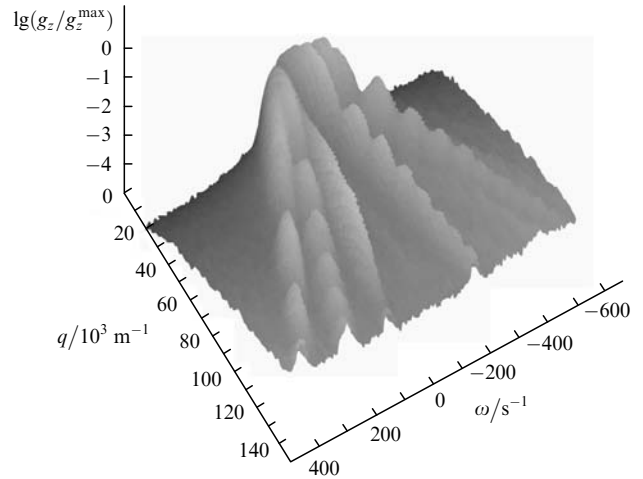


Figure 2. The spatiotemporal intensity spectrum in the sharp-image plane normalised to the maximum value of g_z^{max} .

In the second experiment, the path length, the structural constant and the number of phase screens were increased. The following simulation parameters were specified: $L = 1500$ m, $\lambda = 0.5 \mu\text{m}$, $C_n^2 = 7 \times 10^{-16} \text{m}^{-2/3}$, $a_r = 1$ m, $F_t = 1$ m, $a_t = 15$ cm.

The photodetector was located in the plane of the sharp image at a distance of 0.67 mm from the focal plane and the laser beam was collimated with the initial radius $a_0 = 10$ cm. The propagation of the beam in the atmosphere ($0 \leq x \leq L$) was simulated on a grid of size 512×512 elements with a spatial step of 1 mm. The compression coefficient of the computational grid in the photodetector plane was $L/l \approx 1.5 \times 10^3$. The spectrum was estimated by twenty realisations of the intensity distributions of duration equal to 256 counts with an interval of 0.3 ms. Figure 3b presents the results of the wind velocity profile reconstruction. As in the first experiment the coordinates and velocities of the transverse displacement of phase screens are reconstructed with a good accuracy. The errors do not exceed 50 m over the coordinate and 0.1 m s^{-1} over the velocity.

The results of the numerical experiment show that the proposed algorithm allows one with a good accuracy to reconstruct the wind velocity profile by the statistics of the turbulent intensity fluctuations of laser radiation diffusely scattered by the screen in the sharp-image plane of the receiving telescope. Note that the positions of phase screens used in numerical experiments are not specified with respect to the algorithm of the wind velocity profile reconstruction. Obviously, one should not expect the appearance of

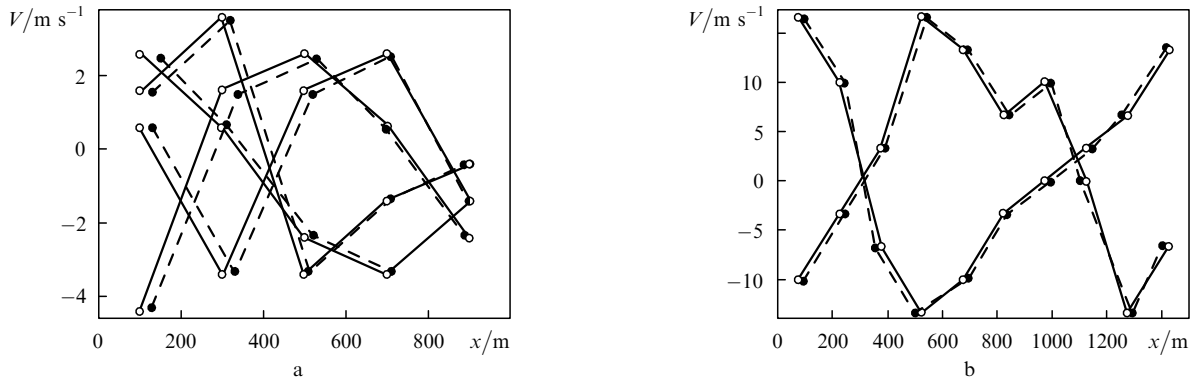


Figure 3. Initial (solid lines, the position of the screens is shown by light points) wind velocity profiles and wind profiles reconstructed by the statistics of intensity fluctuations in the sharp-image plane (dashed lines, the position of screens is shown by dark points): 5 phase screens, $L = 1000$ m (a) and 10 phase screens, $L = 1500$ m (b).

fundamental differences when the algorithm is applied for other points of the path.

5. Conclusions

We have obtained the expressions for the spatiotemporal correlation function of weak random intensity fluctuations of the laser beam diffusely scattered by the screen upon detection of radiation in an arbitrary plane behind the receiving objective. The algorithm has been proposed for reconstructing the wind velocity profile by the statistics of the spatiotemporal spectrum of intensity fluctuations in the sharp-image plane.

The results of numerical experiments on the reconstruction of the velocity and wind direction by computer simulated random realisations of the three-dimensional intensity distributions of the laser radiation diffusely scattered by the screen have been presented. The results of computer experiments show that the developed algorithm allows the wind profile to be reconstructed with the admissible accuracy.

Acknowledgements. The author thanks M.A. Vorontsov for initiating this research and critical remarks. This work was supported by the Technical Research Institute (USA) (Grant No. W911NF-05-1-0552) and the Russian Foundation for Basic Research (Grant Nos 06-05-64445 and 06-05-96951-p-ofi).

References

1. Wang Ting-i, Ochs G.R., Lawrence S. *Appl. Opt.*, **20**, 4073 (1981).
2. Johnston R., Dainty C., Wooder N., Lane R. *Appl. Opt.*, **41**, 6768 (2002).
3. Kluckers V.A., Wooder N.J., Nicholls T.W., Adcock M.J., Munro I., Dainty J.C. *Astron. Astrophys., Suppl. Ser.*, **130**, 141 (1998).
4. Prieur J.-L., Avila R., Daigne G., Vernin J. *Pub. Astron. Soc. Pac.*, **116**, 778 (2004).
5. Avila R., Carrasco E., Ibanez F., Vernin J., Prieur J.-L., Cruz D.X. *Pub. Astron. Soc. Pac.*, **118**, 503 (2006).
6. Garcia-Lorenzo B., Fuensalida J.J. *Mon. Not. R. Astron. Soc.*, **372**, 1483 (2006).
7. Banakh V.A., Marakasov D.A. *Opt. Lett.*, **32** (15), 2236 (2007).
8. Banakh V.A., Marakasov D.A. *J. Opt. Soc. Am. A*, **24** (10), 3245 (2007).
9. Clifford S.F., Ochs G.R., Wang Ting-i. *Appl. Opt.*, **14**, 2844 (1975).
10. Banakh V.A., Marakasov D.A., Vorontsov M.A. *Appl. Opt.*, **46** (33), 8104 (2007).
11. Banakh V.A. *Opt. Atmos. Okean.*, **20** (4), 303 (2007).
12. Banakh V.A., Mironov V.L. *Lokatsionnoe rasprostranenie lazernogo izlucheniya v turbulentnoi atmosfere* (Probe Laser Radiation Propagation in a Turbulent Atmosphere) (Novosibirsk: Nauka, 1986).
13. Charnotskii M.I., Gozani J., Tatarskii V.I., Zavorotny V.U., in *Progress in Optics*. Ed. by E. Wolf (Amsterdam: Elsevier, 1993) Vol. XXXII, p. 203.
14. Panofsky H.A., Dutton J.A. *Atmospheric Turbulence: Models and Methods for Engineering Applications* (New York – Singapore: Wiley Int. Publ., 1983).
15. Banakh V.A., Falits A.V. *Proc. SPIE. Int. Soc. Opt. Eng.*, **4678**, 132 (2001).